https://doi.org/10.15407/ujpe71.8.671

A. JUMABAEV,[1] A. ABSANOV,[1] SH. UMIDULLAYEV,[1] Z. ERNAZAROV,[1]
M. SHOIMOV,[1] M. USMONOV,[1] L. BULAVIN [1, 2]

[1] Sharof Rashidov Samarkand State University
(15, University Blvd., Samarkand 703004, Uzbekistan; e-mail: abduvakhidj@gmail.com)
[2] Taras Shevchenko National University of Kyiv
(64/13, Volodymyrska Str., Kyiv 01601, Ukraine)

VIBRATION SPECTROSCOPY AND QUANTUM-CHEMICAL CALCULATION ANALYSIS OF INTERMOLECULAR INTERACTIONS IN ORTHO-XYLENE AND ITS SOLUTIONS WITH DIMETHYL SULFOXIDE

In this work, the intermolecular interactions in ortho-xylene and its solution in dimethyl sulfoxide (DMSO) were studied using vibrational spectra and quantum chemical calculations. Analysis of Raman spectra showed that DMSO affects the molecular spectral properties of ortho-xylene, which is a result of solvent effects, hydrogen bonding, and π-electron interactions. The mechanisms of molecular cluster formation were studied using density functional theory (DFT) and the B3LYP 6-311++G(d,p) functional set. The calculations allowed us to analyze quantum chemical parameters such as molecular electrostatic potential (MEP), frontier molecular orbitals (HOMO and LUMO), Mulliken charges, electron localization function (ELF), and localized orbital locator (LOL). The results obtained provide insight into the nature of the interaction between ortho-xylene and DMSO molecules and enable a detailed investigation of the formation of molecular clusters in solution. The analysis showed that π-bonds play a key role in the interactions between ortho-xylene and DMSO molecules, leading to the formation of molecular clusters and changes in the properties of spectral lines. This study makes an important contribution to understanding the mechanism of intermolecular interactions in the liquid phase.

K e y w o r d s: Raman, *ab initio* calculations, hydrogen bonding, ortho–xylene, DMSO, molecular electrostatic potential (MEP) surface, FMO, HOMO, LUMO, ELF, LOL.

1. Introduction

The study of Raman spectra shows that intermolecular interactions play a significant role, which leads to changes in the spectral parameters of the interacting molecules. The study of xylene solutions in protic solvents is important, since the formation of complexes changes the proton-acceptor properties of the studied system [1–5]. Xylene (dimethylbenzene, $(CH_3)_2C_6H_4$) consists of a benzene ring substituted with two methyl groups, whose relative positions give rise to three isomers: ortho-, meta-, and para-xylene [6–8]. Complex formation in proton-donor solvents also modifies the proton-acceptor properties of xylene [9]. Chung *et al.* [10] studied ortho-, meta-, and para-xylene, ethylbenzene, toluene, and aliphatic and aromatic hydrocarbons in the process of xylene production using IR spectroscopy. To further characterize xylene and its mixtures, the gas-phase IR spectra of all three isomers in the range of 6500–540 cm^{-1} were measured, and all the principal vibrational frequencies were assigned. Liquid-phase IR and Raman spectra were also studied and calculated using the density functional theory (DFT) [11]. The results of

C i t a t i o n: Jumabaev A., Absanov A., Umidullayev Sh., Ernazarov Z., Shoimov M., Usmonov M., Bulavin L. Vibration spectroscopy and quantum-chemical calculation analysis of intermolecular interactions in ortho-xylene and its solutions with dimethyl sulfoxide. *Ukr. J. Phys.* **71**, No. 8, 671 (2026). https://doi.org/10.15407/ujpe71.8.671.

the Raman experiments and quantum chemical calculations show that the dimeric aggregations of benzene molecules with methyl alcohol and formic acid molecules occur mainly with the participation of the π-electrons of the benzene ring.These complexes are stabilized by intermolecular interactions involving the π-electrons of the benzene ring [12–14]. In our previous work, we studied ortho-xylene and its solution in chloroform, where we found that the symmetric stretching vibration of the CH_3 groups of ortho-xylene with ring symmetry shifts to lower frequencies as the chloroform concentration decreases compared to the pure state. The main reason for this shift is that the hydrogen atom of the CH group of chloroform and the π-electrons in the aromatic ring participate in a CH...π interaction. This leads to a decrease in the vibrational frequency [15].

Understanding the structure of liquids and the intermolecular interactions in the liquid phase is important for detailed understanding of the microscopic aspects of solution formation processes [16]. DMSO ($(CH_3)_2SO$) is a molecule with a C_s symmetry plane containing S and O atoms, which has been used for many years as an important inorganic solvent. The two methyl groups of this molecule are equivalent, and the hydrogen atoms in these groups are located differently with respect to the oxygen and sulfur atoms. The hydrogen atoms of the methyl groups are considered to contribute significantly to the association of DMSO molecules. Due to its rapid penetration through human skin, and its use as a therapeutic agent for arthritis and bursitis, studying the structure of the DMSO molecule is important in the medical field [17, 18].

The properties of xylene liquid mixtures were analyzed using computational chemistry, molecular dynamics, and quantum chemical calculations. Since the intermolecular interactions involving aromatic rings are of great interest, the fundamental and structural features of the intermolecular forces were determined. Molecular clusters, molecular distribution, and mixture dynamics were studied as functions of the mixture composition and temperature, and the results obtained demonstrated the suitability of xylene for applications in the oil and gas industry [19].

The literature review indicates that changes in the spectral line shapes of ortho-xylene–DMSO solutions have not been fully investigated to date. This issue remains important and requires further study. In this paper, various electro-optical and thermodynamic parameters of ortho-xylene–DMSO solutions were analyzed using quantum chemical calculations. In addition, topological analyses, frontier molecular orbital analysis, Mulliken atomic charge analysis, and molecular electrostatic potential (MEP) surface analysis were performed using density functional theory (DFT).

2. Experimental and Theoretical Methods

2.1. Experimental method

The experiments were carried out using liquid mixtures of chemically purified ortho-xylene and DMSO with mole fractions of $0.9, 0.7, 0.5, 0.3$, and 0.1. The samples were further purified according to the methods described in [20].

All experiments were performed at room temperature and normal atmospheric pressure. Raman spectra of ortho-xylene and its solutions with DMSO at various concentrations were recorded using an In-Via Raman spectrometer equipped with a diffraction grating of 1200 lines/mm. The exposure time was 10 s, and the spectral resolution was 0.01 cm^{-1}. A Spectrum Stabilized Laser Module laser with a wavelength of 532 nm and a power of 50 mW was used as the excitation source. The scattered light was recorded using the Renishaw CCD detector.

2.2. Computational method

Quantum chemical calculations were performed using Gaussian 09W [21], the density functional theory DFT/6-311++G(d,p) method and the B3LYP (Becke-3-Lee-Yang-Parr) hybrid functional [22, 23]. Spectra were plotted using Origin 8.5 [24]. The geometric structure of the molecule was visualized using GaussView 6 [25] and VMD [26]. ELF and LOL topological parameters were calculated using Multiwfn 3.8 (Win 64) [27].

3. Results and Discussion

3.1. Raman spectra of ortho-xylene and its solutions with DMSO

Figure 1 shows the experimental results obtained for pure ortho-xylene and its solutions in DMSO. It can be seen from the figure that the Raman scattering spectra of pure ortho-xylene are complex and

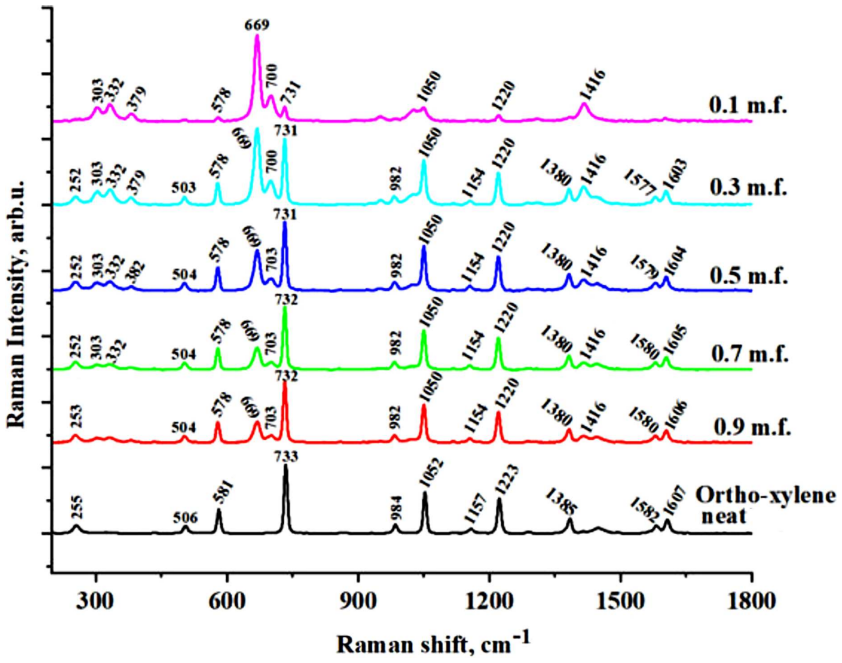

Fig. 1. Raman scattering spectra of pure ortho-xylene and its solutions in DMSO in the range of 200–1800 cm^{-1} (the concentration is given as the mole fraction of ortho-xylene)

exhibit several vibrational maxima. In pure ortho-xylene, the spectral band corresponding to the C–H vibration of the CH_3 group is located at 255 cm^{-1}, and in solution in DMSO, this spectral line shifts to 252 cm^{-1}. The C–H symmetric vibration of ortho-xylene at 733 cm^{-1} is shifted to a lower frequency under the influence of DMSO, and with a decrease in the ortho-xylene concentration in the mixture and an increase in the DMSO content, this shift continues to 731 cm^{-1}. The spectral lines at 1157 cm^{-1} and 1223 cm^{-1} correspond to the HCC and CCC deformation vibrations of the ring, and in the presence of DMSO, both vibrations shift to lower frequency by 3 cm^{-1}, respectively. Similarly, the spectral line at 1607 cm^{-1}, which corresponds to the deformational CC vibration of the ortho-xylene ring, shifts to a lower frequency by up to 4 cm^{-1} with increasing DMSO content in the solution (1606 cm^{-1} at 0.9 m.f., 1605 cm^{-1} at 0.7 m.f., 1604 cm^{-1} at 0.5 m.f., and 1603 cm^{-1} at 0.3 m.f.) (Fig. 1). The main reason for such changes is the solvent effect. DMSO surrounds the ortho-xylene molecules and interferes with their free vibrations. This causes the C–H bond to be shortened, which reduces the vibrational frequency.

Figure 2 shows the Raman spectra of ortho-xylene and its solutions in DMSO in the vibrational frequency range 2800–3200 cm^{-1}. It can be observed that C–H vibration of the CH_3 group of pure ortho-xylene, which occurs at 2919 cm^{-1}, shifts to a lower frequency and reaches 2912 cm^{-1} with increasing DMSO content in the mixture. The shift of the 2919 cm^{-1} line in the Raman spectrum to a lower frequency is observed as a result of interaction of the C–H bonds of the methyl group of DMSO with the π electrons of ortho-xylene. The spectral line corresponding to the 3044 cm^{-1} vibration of ortho-xylene shifts to a lower frequency, reaching 3041 cm^{-1} with increasing DMSO concentration, i.e., by 3 cm^{-1} with decreasing ortho-xylene concentration in the solution. This vibration band is not observed when the concentration of ortho-xylene in the solution decreases to 0.1 m.f. Experiments show that in solutions of pure ortho-xylene with DMSO, a shift of the spectral lines to lower frequency was observed. The main reason for this shift may be the formation of CH$\cdots\pi$ interactions between the hydrogen atom of DMSO and the π-electrons of the aromatic ring of ortho-xylene.

3.2. Molecular electrostatic potential (MEP)

Molecular electrostatic potential (MEP) is useful for visualizing the charge distribution in ortho-xylene

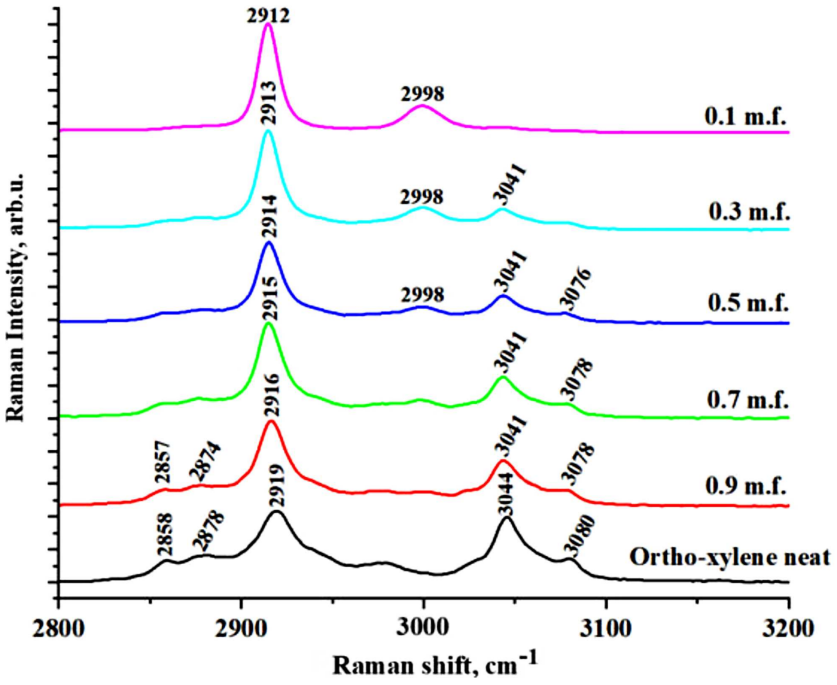

Fig. 2. Raman scattering spectra of pure ortho-xylene and its solutions in DMSO in the range of 2800–3200 cm^{-1} (concentrations are given as mole fractions of ortho-xylene)

and its DMSO complexes, as well as for studying charge-dependent parameters such as electrophilic and nucleophilic processes and binding. Different colors on the molecular electrostatic potential (MEP) surface help to identify the reactive regions of the molecule [28–32]. Figure 3 depicts the MEP using different color classifications. It is represented in different colors depending on the magnitude of electrostatic potential. Orange < yellow < green < blue is shown in the order of increasing electrostatic potential [33, 34]. Molecular electrostatic potential or molecular potential surface mapping visually represents the charge distribution in ortho-xylene monomers, dimers and ortho-xylene + DMSO complexes. Charge-dependent parameters play an important role in the study of electrophilic, nucleophilic reactions and bonds, while another purpose of finding the electrostatic potential is to identify the reactive sites of the molecule. The MEP map from –2.678 e^{-2} eV to 2.678 e^{-2} eV shows that the ring center in the monomer of ortho-xylene has a negative potential. The red color corresponds to the electrophilic region, which is associated with the largest negative charge of the molecule. The yellow color around the C–H group located along the ring is a slightly electron-rich region whereas the green color represents zero potential. The blue color around CH3 indicates that the nucleophilic part is positively charged. When the MEP map given in the range –2.669 $e^{-2} \div 2.66\, e^{-2}$ eV is viewed for the ortho-xylene dimer complex, we can see that the hydrogen atom in the CH_3 group of ortho-xylene is directed towards the ring center of the second ortho-xylene, and the colors in the MEP also indicate that the dimer is formed through this type of interaction. When we look at the ortho-xylene + 1DMSO complex, the hydrogen atoms in the CH_3 groups of ortho-xylene form a bond through the oxygen atom in the S=O group of DMSO (–5.182 $e^{-2} \div 5.182$ e^{-2} eV). The highest MEP potential of the ortho-xylene + 2DMSO complex was found to be (–6.730 $e^{-2} \div 6.730$ e^{-2} eV).

3.3. Frontier Molecular Orbital (FMO) Analysis

The electronic properties and reactivity of molecules can be explained by examining their frontier molecular orbitals, i.e. the highest occupied molecular orbital (HOMO) and the lowest unoccupied molecular orbital (LUMO). These orbitals are the outermost regions of the electronic structure of a molecule and play a crucial role in various chemical processes, es-

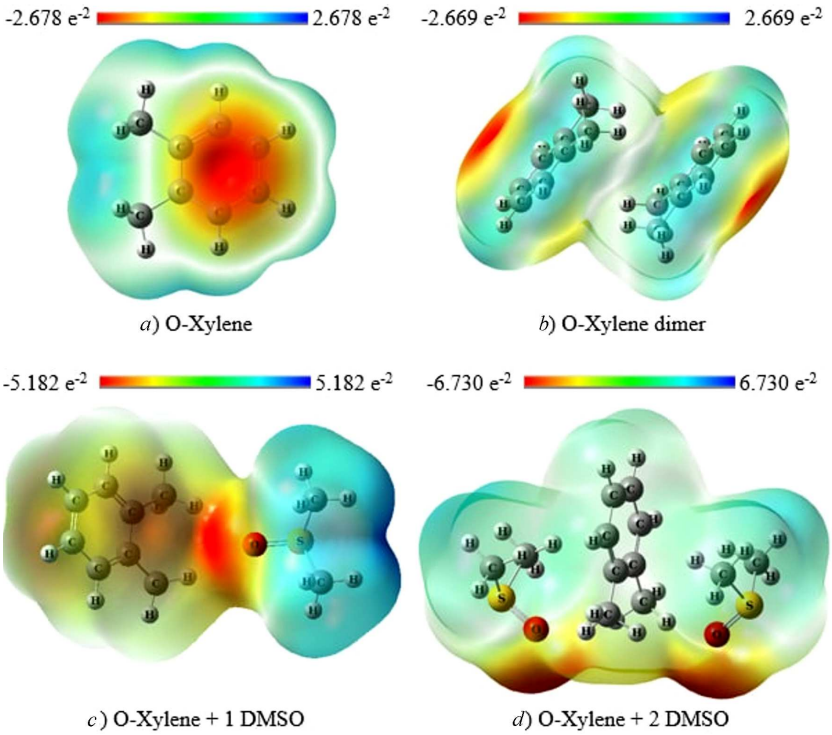

Fig. 3. MEP Diagram for ortho-xylene + DMSO complexes

pecially those involving electron transfer. The HOMO is primarily important for electron-donating or nucleophilic reactions. A molecule with a relatively high energy HOMO is usually a good electron donor and can easily participate in oxidation or nucleophilic reactions. In contrast, the LUMO represents the lowest-energy orbital available for electron occupation, i.e., an electron-occupied or empty molecular orbital. Molecules with low LUMO energies are generally good electron acceptors and can participate in electrophilic reactions [35–38]. The energy difference between the HOMO and LUMO is often an important characteristic of molecular reactivity. A smaller HOMO–LUMO energy gap means that the molecule is more easily excited, making it more reactive.

Figure 4 presents the HOMO–LUMO visualization of ortho-xylene and its complexes with DMSO. Table 1 presents the FMO-derived properties based on the energy gap data, including the electrophilicity index, chemical hardness, chemical softness, and electronegativity of the complexes, and the thermodynamic and chemical parameters in ortho-xylene and its solutions in DMSO, as well as the parameters determined by the HOMO and LUMO energy difference. According to Table 1, the dipole moment for the ortho-xylene + DMSO complex is larger than that of the monomer.

The vibrational energy and HOMO–LUMO energy difference are the largest for the ortho-xylene monomer (144.6709 kcal/mol). For the ortho-xylene dimer, it is 141.7443 kcal/mol. For the ortho-xylene + 1DMSO complex, it is 127.1736 kcal/mol whereas for the ortho-xylene + 2DMSO complex, it is 137.1659 kcal/mol. The ionization potential values are 151.3151 kcal/mol (ortho-xylene monomer), 150.852 kcal/mol (ortho-xylene dimer), 140.1001 kcal/mol (ortho-xylene + 1DMSO), and 146.949 kcal/mol (ortho-xylene + 2DMSO). The electrophilicity index is highest for the ortho-xylene + + 1DMSO complex (46.03656 kcal/mol).

3.4. Mulliken charge distribution of ortho-xylene and DMSO complexes

Mulliken atomic charge analysis using quantum chemical calculations plays an important role in explaining the molecular behavior of complexes, as atomic

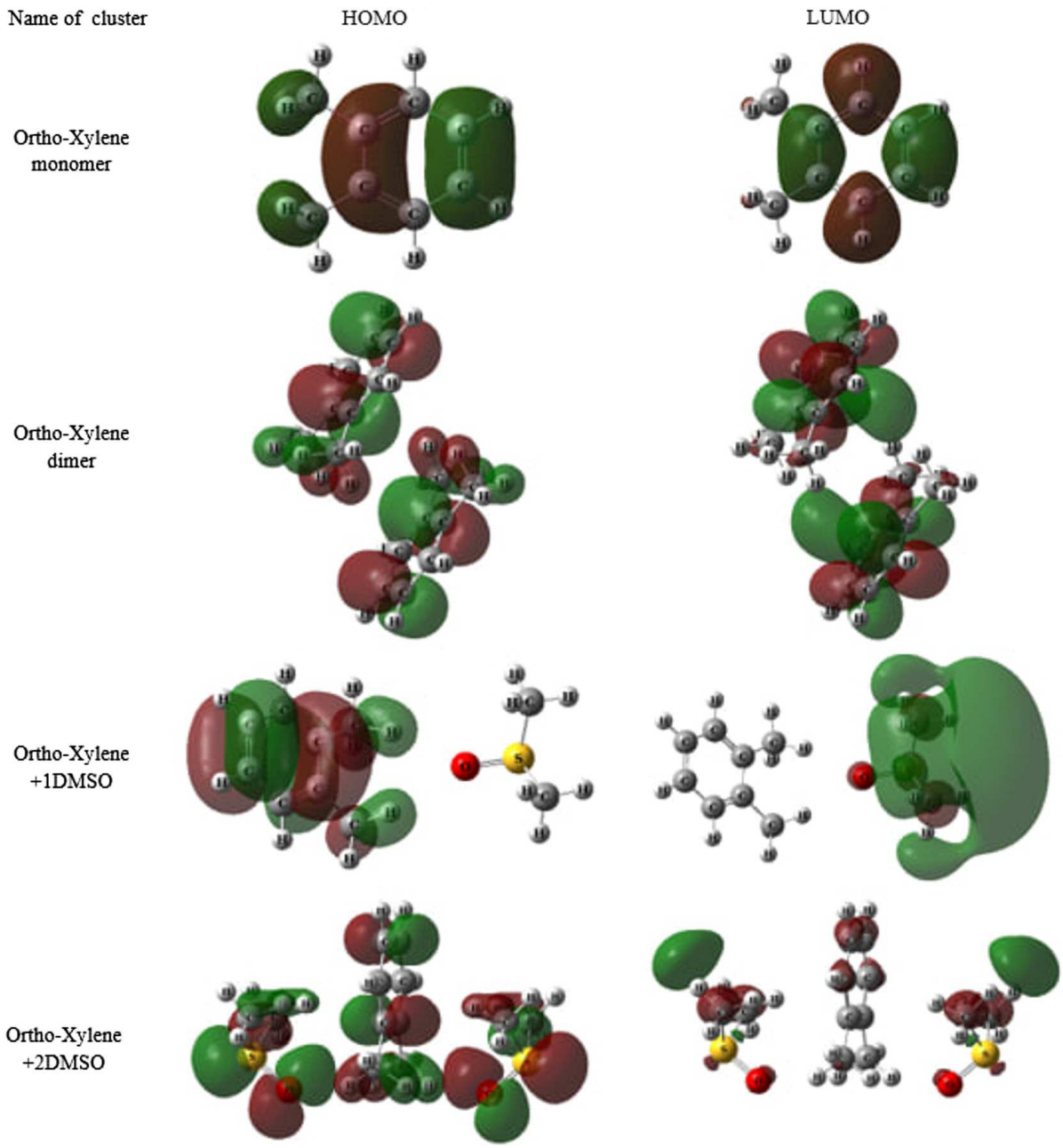

Fig. 4. Frontier molecular orbital diagram of ortho-xylene and its solutions

charges affect a number of molecular properties, including electronic structure, reactivity, dipole moment, polarization, and vibrational spectra [39]. Table 2 presents the Mulliken charge distributions for the ortho-xylene monomer, dimer, and DMSO complexes.

Figure 5 shows the Mulliken charge distributions for these complexes. These distributions play an important role in charge transfer between the interacting parts of the molecules. In the ortho-xylene monomer, dimer, and DMSO complexes, C^1, C^2, and all hydrogen atoms are positively charged, whereas

Table 1. **Thermodynamical and chemical parameters of title compounds**

Parameters	Ortho-xylene monomer	Ortho-xylene dimer	Ortho-xylene + + 1DMSO	Ortho-xylene + + 2DMSO
Dipole moment (Debye) μ	0.6758	0.0022	5.94725	6.186403
Total energy (thermal) (kcal/mol)	102.038	205.857	155.752	211.951
Zero-point vibrational energy (kcal/mol)	97.262	194.686	147.076	197.34149
E_{HOMO}	–151.315	–150,852	–140.1001	–146.949
E_{LUMO}	–6.6465	–9.10584	–12.9286	–9.78277
$E_{\mathrm{LUMO}} - E_{\mathrm{HOMO}}$	144.6709	141.7443	127.1736	137.1659
Global hardness $(\eta) = (E_{\mathrm{LUMO}} - E_{\mathrm{HOMO}})$	72.3343	70.8722	63.5868	68.58294
Chemical potential $(\mu) = (E_{\mathrm{LUMO}} + E_{\mathrm{HOMO}})$	–78.9808	–79.9771	–76.5154	–78.3657
IP $= -E_{\mathrm{HOMO}}$	151.3151	150.852	140.1001	146.949
EA $= -E_{\mathrm{LUMO}}$	6.646497	9.10492	12.92861	9.78277
Electrophilicity index $(\omega) = \mu^2/2\eta$	43.11921	45.1279	46.03656	44.77196

Table 2. **Mulliken charge distribution of ortho-xylene**

Atomic number	Mulliken charge distribution (in electron units)			
	Ortho-xylene monomer	Ortho-xylene dimer	Ortho-xylene + + 1DMSO	Ortho-xylene + + 2DMSO
C^1	0.572404	0.415232	0.698069	0.609991
C^2	0.572409	0.406453	0.913015	0.610744
C^3	–0.536144	–0.163701	–0.639400	–0.047164
C^4	–0.536142	–0.166121	–0.563627	–0.047254
C^5	–0.588616	–0.705441	–0.720399	–1.011951
C^6	–0.588615	–0.711636	–0.683802	–1.011350
C^7	–0.172530	–0.333694	–0.236691	–0.451245
C^8	–0.172529	–0.333461	–0.228040	–0.451458
H^9	0.115429	0.149043	0.119858	0.171806
H^{10}	0.115429	0.148487	0.120417	0.171707
H^{11}	0.147833	0.148576	0.124377	0.227981
H^{12}	0.147735	0.192742	0.147285	0.228685
H^{13}	0.156311	0.142785	0.148744	0.124767
H^{14}	0.147700	0.148062	0.196524	0.228399
H^{15}	0.156311	0.142953	0.144911	0.124800
H^{16}	0.147868	0.193200	0.142850	0.227722
H^{17}	0.157574	0.163239	0.152411	0.165374
H^{18}	0.157574	0.163223	0.152109	0.165409

the C^3, C^4, C^5, C^6, C^7, and C^8 atoms are negatively charged.

During complex formation, the electron density at the H^{12} hydrogen atom in the CH_3 group increases dramatically due to the charge transfer between the hydrogen atom and the oxygen atom of DMSO. The charge on the carbon atom changes from 0.147735e in the monomer to 0.228685e in the ortho-xylene + + 2DMSO complex. Similarly, the charge on the carbon atom (C^5) in the CH_3 group involved in the bonding decreases from –0.588616e to –1.011951e (ortho-xylene + 2DMSO) (Table 2). Such changes in the charge distribution lead to an increase in the bond length of the CH_3 group, resulting in changes in the vibrational frequencies at different solvent concentrations.

For the ortho-xylene + 2DMSO complex, the atomic charges of H^{12} and H^{14} increase, whereas the absolute values of the charges on H^{13} and H^{15} decrease. Figure 5 shows that the charge distribution for the complexes ortho-xylene + 1DMSO and ortho-xy-

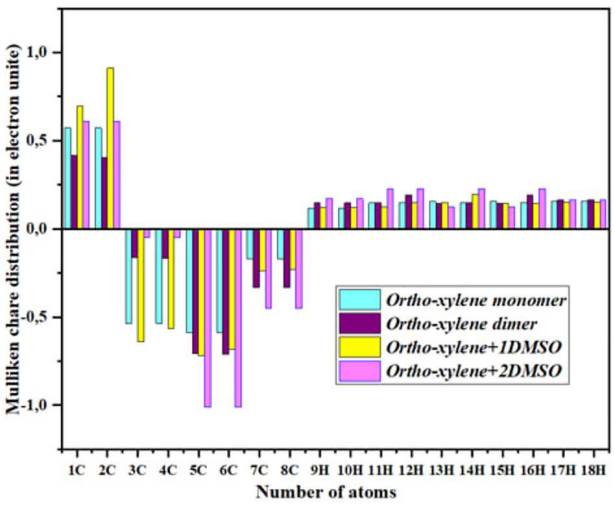

Fig. 5. Mulliken charge distributions of ortho-xylene + DMSO complexes

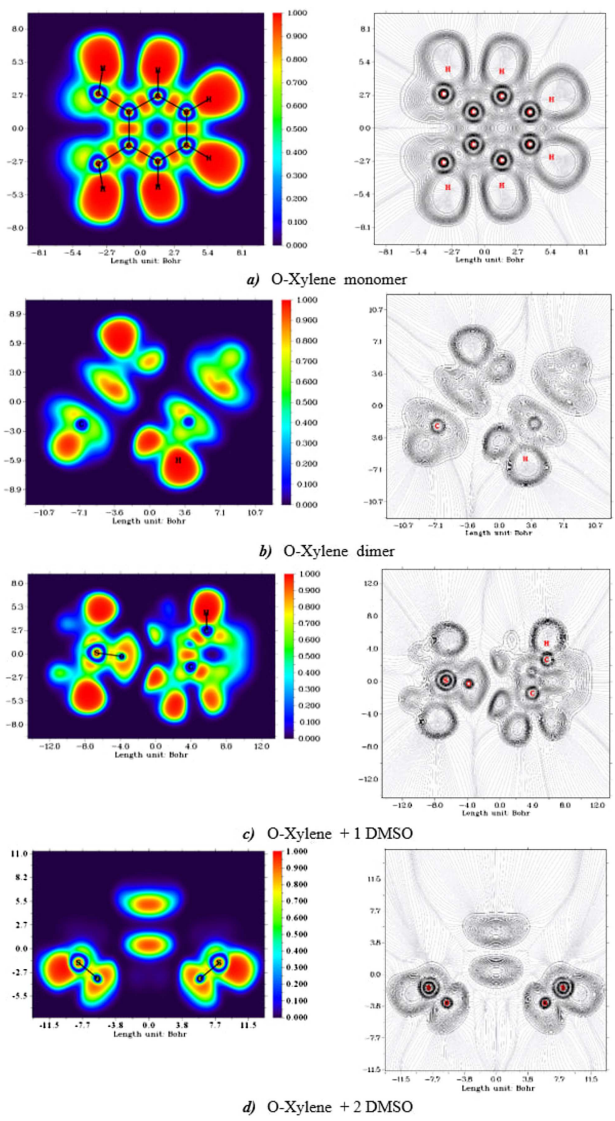

Fig. 6. LOL maps of the studied complexes

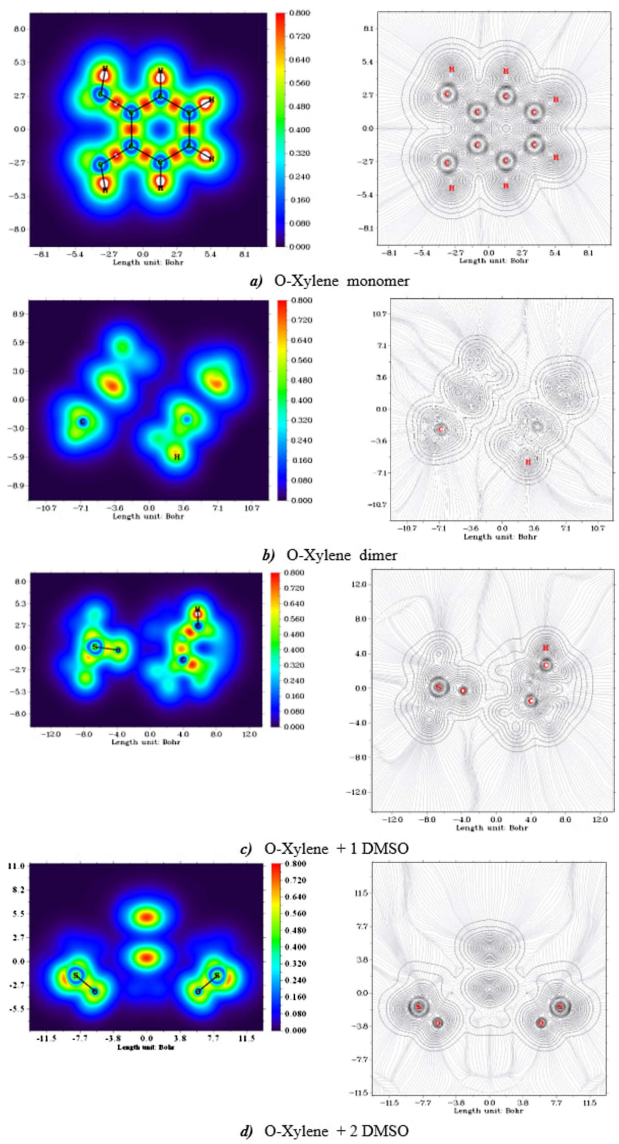

Fig. 7. LOL maps of the studied complexes

lene + 2DMSO is also modified, and this change is significant for the atoms participating in the interaction.

3.5. ELF and LOL analyses

Electron localization function (ELF) and localized orbital locator (LOL) analyses are widely used to describe chemical bonding in atomic and molecular systems and to identify regions of electron localization [40]. Whereas ELF describes the localization of paired electrons, LOL describes the maximum localized orbitals that overlap each other due to the gradient of orbitals. The maximum number of electron pairs in the space between molecules due to covalent bonding forms the main line of ELF and LOL maps [41, 42]. Figures 6 and 7 show ELF and LOL color maps for ortho-xylene monomer (a), ortho-xylene dimer (b), and ortho-xylene + 1DMSO (c), ortho-xylene + 2DMSO (d) complexes. The color values on the y-axis are given on a scale from blue to red, with ELF values ranging from 0 to 1.0 and LOL values ranging from 0 to 0.8. Both ELF and LOL have an interval scale, representing bound and unbound localized electron bands ranging from 0.5 to 1.0.

Delocalized electrons are indicated by regions where the ELF or LOL values are <0.5. Red and orange colors correspond to high electron localization. The region between the core and valence shells is represented by a blue area. In the ELF and LOL maps, red corresponds to the highest localization values, indicating the presence of both bonded and unbonded electrons. The red color area with high ELF or LOL values shown around hydrogen atoms indicates a lone pair of electrons due to covalent bonding or high localization of electrons due to the presence of a nuclear shell in this area.

4. Conclusions

The presence of interactions between ortho-xylene and DMSO and the resulting spectral line shifts due to solvent effects, hydrogen bonding and π-electrons were observed. Raman spectra of ortho-xylene/DMSO binary mixtures with concentrations of 0.9, 0.7, 0.5, 0.3 and 0.1 mole fractions were studied. In pure ortho-xylene, the spectral band corresponding to the C–H vibration of the CH_3 group was observed at 255 cm^{-1}, and in solution in DMSO, this spectral line was found to be at 252 cm^{-1}, corresponding to a red shift of 3 cm^{-1}. The spectral lines corresponding to the HCC and CCC ring deformation vibrations were observed at 1157 cm^{-1} and 1223 cm^{-1}, and in solution with DMSO, both vibrations were shifted to lower frequencies, respectively. The shift of the 2919 cm^{-1} line in the Raman spectrum to a lower frequency is observed as a result of the interaction of the C-H vibration of the methyl group of DMSO with the π-electrons of ortho-xylene in the solvent environment (solvation effect). The main reason for this shift to a lower frequency is the formation of CH$\cdots\pi$ interactions between the hydrogen in the CH group of DMSO and the π electrons of the aromatic ring of ortho-xylene.

The formation mechanisms of molecular clusters of ortho-xylene and its solutions with DMSO were studied using density functional theory (DFT) and B3LYP 6-311++G (d,p) functional set. The charge transfer on each atom during the complex formation was analyzed and the thermodynamic parameters were studied. The structural parameters of the molecules, molecular electrostatic potential (MEP), electronic properties and reactivity of the molecules were investigated by calculating their frontier molecular orbitals, i.e. the highest occupied molecular orbital (HOMO) and the lowest unoccupied molecular orbital (LUMO). Mulliken atomic charges, Electron Localization Functions (ELF) and Localized Orbital Locator (LOL) analyses were performed using the DFT method. These topological analyses provide insight into the intermolecular interactions and bonding between the interacting molecules.

This work was supported by Project No. FZ20200929385 of the Ministry of Higher Education, Science and Innovation of the Republic of Uzbekistan.

1. M. Nishio, Y. Umezawa, J. Fantini, M. Weiss P. Chakrabarti. CH-π hydrogen bonds in biological macromolecules. *Phys. Chem. Chem. Phys.* **16** (25), 12648 (2014).
2. L. Xu, X. Miao, X. Ying, W. Deng. Two-dimensional self-assembled molecular structures formed by the competition of van der Waals forces and dipole–dipole interactions. *J. Phys. Chem. C* **116** (1), 1061 (2012).
3. M. Sinnokrot, D. Sherrill, High-accuracy quantum mechanical studies of $\pi-\pi$ interactions in benzene dimers. *J. Phys. Chem. A* **110** (37), 10656 (2006).
4. A. Jumabaev, A. Absanov, Z. Ernazarov, A. Shodiyev, S. Umarov. Raman spectra and ab-initio calculation analysis of intermolecular interactions in ethyl acetate. *J. Samarkand State Univ.* **139** (1), 5 (2023).
5. A. Jumabaev, A. Absanov, B. Khudaykulov, Z. Ernazarov. Investigation of intermolecular interactions in butyl acetate using vibrational spectroscopy and nonempirical calculations. *Uzbek Phys. J.* **25** (4), (2023).
6. P. Alvarez, M. Vogel. Substrate interactions of benzene, toluene, and para-xylene during microbial degradation by pure cultures and mixed culture aquifer slurries. *Appl. Environ. Microbiol.* **57**, 2981 (1991).
7. E. Edwards, L. Wills, M. Reinhard, D. Grbić-Galić. Anaerobic degradation of toluene and xylene by aquifer microorganisms under sulfate-reducing conditions. *Appl. Environ. Microbiol.* **58**, 794 (1992).
8. C. Eberhardt, P. Grathwohl. Time scales of organic contaminant dissolution from complex source zones: coal tar pools vs. blobs. *J. Contam. Hydrol.* **59**, 45 (2002).
9. S. Naganandhini, T. Sangeetha, G. Arivazhagan. FTIR Spectroscopic studies on the binary solutions of 1–propanol with xylene isomers. *Orient. J. Chem.* **37** (3), 710 (2021).
10. H. Chung, J. Lee, M. Ku. Feasibility of simultaneous measurement of xylene isomers and other hydrocarbons in p-xylene production processes using near-infrared spectroscopy. *Appl. Spectr.* **52**, 885 (1998).
11. R. Lindenmaier, N. Scharko, R. Tonkyn, K. Nguyen, S. Williams, T. Johnson. Improved assignments of the vibrational fundamental modes of ortho-, meta-, and para-

xylene using gas- and liquid-phase infrared and Raman spectra combined with ab initio calculations: Quantitative gas-phase infrared spectra for detection. *J. Mol. Struct.* **1149**, 332 (2017).
12. F. Tukhvatullin, A. Jumabaev, U. Tashkenbaev, H. Hushvaktov, A. Absanov, G. Sharifov. Aggregation of benzene molecules with molecules of methanol and formic acid. *Ukr. J. Phys.* **57** (2), 244 (2012).
13. F. Tukhvatullin, A. Jumabaev, H. Hushvaktov, A. Absanov, G. Sharifov. On proton acceptor and proton donor properties of benzene molecules. *J. Rep. Acad. Sci.* No. 4, 25 (2011).
14. A. Jumabaev, G. Sharifov, H. Hushvaktov, A. Amonov. Studying the processes of intermolecular interactions in xylene solutions by spectra of Raman scattering and ab initio calculations. *Open Access J. Phys.* **3** (3), 10 (2019).
15. A. Fujii, S. Morita, M. Miyazaki, T. Ebata, N. Mikami. A molecular cluster study on activated CH/π interactions: Infrared spectroscopy of aromatic molecule? Acetylene clusters. *The J. Phys. Chem. A* **108** (14), 2652 (2004).
16. B. Marekha, K. Sonoda, T. Uchida, T. Tokuda, A. Idrissi, T. Takamuku. Intermolecular studies in molecular liquids. *J. Mol. Liq.* **232**, 431 (2017).
17. R. Thomas, C. Shoemaker, K. Eriks. Crystal structure studies. *Acta Cryst.* **21**, 12 (1966).
18. H. Torii, M. Tasumi. Vibrational analysis studies. *Bull. Chem. Soc. Jpn.* **68**, 128 (1995).
19. A. Gutiérrez, M. Atilhan, S. Aparicio. Nanoscopic approach on benzene-toluene-xylenes extraction by sulfolane. *J. Mol. Liq.* **249**, 1039 (2018).
20. A. Gordon, R. Ford. *The Chemist's Companion: A Handbook of Practical Data, Techniques, and References* (Wiley, 1973).
21. A. Becke. Density-functional thermochemistry. III. The role of exact exchange. *J. Chem. Phys.* **98** (7), 5648 (1993).
22. C. Lee, W. Yang, R. Parr. Development of the Colle–Salvetti correlation-energy formula into a functional of the electron density. *Phys. Rev. B* **37** (2), 785 (1988).
23. M. Frisch, G. Trucks, H. Schlegel *et al. Gaussian 09, Revision D.1* (Gaussian, Inc., Wallingford, 2009).
24. J. Moberly, M. Bernards, K. Waynant. Key features and updates for Origin. *J. Cheminform.* **10**, Article 5 (2018).
25. R. Dennington, T. Keith, J. Millam. *GaussView Version 6* (Semichem Inc., 2016).
26. W. Humphrey, A. Dalke, K. Schulten. VMD: Visual molecular dynamics. *J. Mol. Graph.* **14** (1), 33 (1996).
27. T. Lu, F. Chen. Multiwfn: A multifunctional wavefunction analyzer. *J. Comput. Chem.* **33**, 580 (2012).
28. J. Murray, K. Sen. *Molecular Electrostatic Potentials: Concepts and Applications* (Elsevier, 1996).
29. A. Jumabaev, B. Khudaykulov, U. Holikulov, A. Norkulov, J. Subbiah, O. Al-Dossary, N. Issaoui. Molecular structure, vibrational spectral assignments, MEP, HOMO–LUMO, AIM, NCI, RDG, ELF, LOL properties of acetophenone and for its solutions based on DFT calculations. *Optical Materials* **159**, 116683 (2025).
30. N. Chetry, T. Devi. Intermolecular interaction study of L-Threonine in polar aprotic solvent: Experimental and theoretical study. *J. Mol. Liq.* **338**, 116689 (2021).
31. A. Jumabaev, H. Hushvaktov, A. Absanov, B. Khudaykulov, Z. Ernazarov, L. Bulavin. Vibrational spectra and computational study of amyl acetate: MEP, AIM, RDG, NCI, ELF, and LOL analysis. *Ukr. J. Phys.* **69**, 742 (2024).
32. A. Jumabaev, S. Koyambo-Konzapa, H. Hushvaktov, A. Absanov, B. Khudaykulov, U. Holikulov, M. Nsangou. Intermolecular interactions in water and ethanol solution of ethyl acetate: Raman, DFT, MEP, FMO, AIM, NCI-RDG, ELF, and LOL analyses. *J. Mol. Model.* **30** (10), 349 (2024).
33. S. Koyambo-Konzapa, S. Aljazzar, G. Kongbonga *et al.* Hydration effects on molecular structure, vibrational, electronic properties, drug-likeness analysis, molecular docking, and molecular dynamics studies. *J. Mol. Liq.* **410**, 125609 (2024).
34. A. Jumabaev, H. Hushvaktov, A. Absanov, I. Doroshenko, B. Khudaykulov, L. Djumanov, Z. Ernazarov. Insights into amyl acetate–chloroform interactions: Vibrational spectroscopy and quantum topology study. *Ukr. J. Phys.* **71** (1), 28 (2026).
35. N. Elangovan, S. Al-Hussain, S. Sowrirajan, M. Zaki, S. Gomha, A. Norkulov, Z. Ernazarov. Electronic structure, absorption, and cyclic voltammetry studies of bisimine schiff base: A combined experimental and theoretical correlation. *J. Fluorescence* 1 (2026).
36. A. Jalbout, A. Hameed, B. Trzaskowski. Study of the structural and electronic properties of 1-(4,5 and 6-selenenyl derivatives-3-formyl-phenyl) pyrrolidinofullerenes. *J. Organomet. Chem.* **692**, 1039 (2007).
37. B. Khudaykulov, A. Norkulov, U. Holikulov, A. Absanov, I. Doroshenko, A. Jumabaev. Raman and DFT study of non-covalent interactions in liquid benzophenone and its solutions. *Low Temp. Phys.* **51** (2), 220 (2025).
38. V.F. Korolovych, O.A. Grishina, O.A. Inozemtseva, A.V. Selifonov, D.N. Bratashov, S.G. Suchkov, L.A. Bulavin, O.E. Glukhova, G.B. Sukhorukov, D.A. Gorin. Impact of high-frequency ultrasound on nanocomposite microcapsules: *In silico* and *in situ* visualization. *Phys. Chem. Chem. Phys.* **18** (4), 2389 (2016).
39. B. Shainyan, N. Chipanina, T. Aksamentova, L. Oznobikhina, G. Rosentsveig, I. Rosentsveig. Intramolecular hydrogen bonds in the sulfonamide derivatives of oxamide, dithiooxamide, and biuret. FT-IR and DFT study, AIM and NBO analysis. *Tetrahedron* **66** (44), 8551 (2010).
40. A. Jumabaev, H. Hushvaktov, B. Khudaykulov, A. Absanov, M. Onuk, I. Doroshenko, L. Bulavin. Formation of hydrogen bonds and vibrational processes in dimethyl sulfoxide and its aqueous solutions: Raman spectroscopy and ab initio calculations. *Ukr. J. Phys.* **68** (6), 375 (2023).
41. A. Kazachenko *et al.* Experimental and theoretical study of the sulfamic acid–urea deep eutectic solvent. *J. Mol. Liq.* **363**, 119859 (2022).

42. J. Deephlin Tarika, X. Divya Dexlin, S. Madhankumar, D. Deva Jayanthi, T. Joselin Beaula. Tuning the computational evaluation of spectroscopic, ELF, LOL, NCI analysis and molecular docking of novel anti-COVID-19 molecule 4-dimethylamino pyridinium 3,5-dichlorosalicylate. *Spectrochim. Acta A* **259**, 119907 (2021).

Received 06.04.26

А. Жумабаєв, А. Абсанов, Ш. Умідуллаєв, З. Ерназаров, М. Шоімов, М. Усмонов, Л. Булавін

КОЛИВАЛЬНА СПЕКТРОСКОПІЯ ТА КВАНТОВО-ХІМІЧНИЙ РОЗРАХУНКОВИЙ АНАЛІЗ МІЖМОЛЕКУЛЯРНИХ ВЗАЄМОДІЙ В ОРТО-КСИЛОЛІ ТА ЙОГО РОЗЧИНАХ З ДИМЕТИЛСУЛЬФОКСИДОМ

У цій роботі досліджено міжмолекулярні взаємодії в ортоксилолі та його розчині з диметилсульфоксидом (DMSO) за допомогою аналізу коливальних спектрів і квантово-хімічних розрахунків. Аналіз спектрів комбінаційного розсіювання показав, що DMSO впливає на молекулярні спектральні властивості орто-ксилолу, що є результатом впливу розчинника, водневих зв'язків і π-електронних взаємодій. Механізми утворення молекулярних кластерів досліджувалися в рамках теорії функціонала густини (DFT) за допомогою функціонального набору B3LYP 6-311++G(d,p). Розрахунки дали змогу проаналізувати такі квантово-хімічні параметри, як молекулярний електростатичний потенціал (MEP), граничні молекулярні орбіталі (HOMO і LUMO), заряди за Маллікеном, функція локалізації електронів (ELF) і локатор локалізованих орбіталей (LOL). Отримані результати допомагають зрозуміти природу взаємодії між молекулами орто-ксилолу й DMSO та уможливлюють детальне вивчення формування молекулярних кластерів у розчині. Аналіз показав, що π-зв'язки відіграють головну роль у взаємодії між молекулами орто-ксилолу та DMSO, що спричиняє утворення молекулярних кластерів і зміни властивостей спектральних ліній. Це дослідження робить важливий внесок у розуміння механізму міжмолекулярних взаємодій у рідинній фазі.

Ключові слова: спектри комбінаційного розсіювання, *ab initio* розрахунки, водневий зв'язок, орто-ксилол, DMSO, поверхневий молекулярний електростатичний потенціал (MEP), FMO, HOMO, LUMO, ELF, LOL.